A Diagnostic Analysis of the Simulated Structure of a Meiyu Front System in 1999*

CUI Xiaopeng[1](崔晓鹏), GAO Shouting[1](高守亭), ZHANG Haixia[2](张海霞), and HAO Shifeng[3](郝世峰)

1 *LACS, Institute of Atmospheric Physics, Chinese Academy of Sciences, Beijing* 100029

2 *Handan Meteorological Bureau, Handan* 056001

3 *Zhejiang Institute of Meteorology, Hangzhou* 310017

(Received October 15, 2008)

ABSTRACT

A numerical simulation of a torrential rain event occurring in the Jiang-Huai Valley of China from 22–24 June 1999 is performed and analyzed by using the PSU/NCAR MM5 mesoscale non-hydrostatic model. The high-resolution model output data are utilized to diagnose the double front structure, and the distributions of potential temperature, equivalent potential temperature, and specific humidity in the vicinity of the Meiyu Front System (MYFS) in the Jiang-Huai Valley. The results show that both the potential temperature gradient and the specific humidity gradient have important impacts on the two strong equivalent potential temperature gradient zones associated with the double front structure of the MYFS, but the latter (mois ture gradient) is more important. In addition, the tendency equation of specific humidity gradient is theoretically derived. It shows that variations of the specific humidity gradient are related to the advection, convergence/divergence, horizontal and vertical vorticities (secondary circulation) effects and the gradient of water vapor source/sink. As an example, the budget of the meridional component of the tendency equation is selected and diagnosed by using the above model simulation data of the torrential rain event. It is shown that the variation of the specific humidity gradient averaged throughout the simulation is mainly controlled by the convergence/divergence effect, the secondary circulation effect associated with the horizontal vorticities, and the water vapor source/sink effect. Since the water vapor source/sink is often formed from the phase change processes of water vapor in the air and thus directly associated with cloud and precipitation microphysics processes, the variation of the specific humidity gradient is closely related with cloud and precipitation microphysics and the distribution, development and evolution of cloud and rainfall systems. The double front structure of the MYFS provides an advantageous environmental condition for the development and movement of the mesoscale torrential rain system nearby. In turn, the development of the torrential rain exerts a signifiant impact on the MYFS through changing the thermal and moisture distributions.

Key words: Meiyu Front System(MYFS), the double front structure, specific humidity gradient, tendency equation

1. Introduction

In the summer monsoon season, there often exists a rain belt from the middle and lower Yangtze Valley to southwestern Japan for several weeks, leading to heavy rain events, which is in general called Meiyu in China. Meiyu has always been one of the important meteorological phenomena and research topics in East Asia, especially in China, Japan and South Korea. Early studies showed that Meiyu mainly consists of a quasi-stationary front in the west-east direction and heavy rainfall systems in the vicinity of the front. The quasi-stationary front is called the Meiyu front. Many investigations have focused on the front (Akiyama, 1973, 1975; Gao et al., 1990, 2002; Matsumoto et al., 1970, 1971; Ninomiya, 1999; Shou et al., 2001; Cui et al., 2003a, b; Cui, 2001; Yan et al., 2005; Ni and Zhou, 2004; Qin et al., 2004). Their results showed that (1) there exists a distinct contrast of humidity across the front, and the gradient of equivalent potential temperature rather than temperature should be used to represent the front; (2) the Meiyu front is a subtropical frontal system with multi-scale features along which convections are active. The Meiyu front covers the eastern parts of mainland China, the East China Sea, Japan, and the North Pacific from west to

*Supported by the National Natural Science Foundation of China under the Grant No. 40505012, 40433007, and the Knowledge Innovation Program of the Chinese Academy of Sciences (IAP07214).

Corresponding author: xpcui@mail.iap.cn.

east. It is one of the most important hydrological cycling systems in East Asia. The Meiyu front is much different from other typical mid-latitude fronts due to its distinct gradient of humidity and relatively weaker gradient of temperature in the south-north direction.

Many researchers studied the structure of the moist layer and transportation of water vapor near the Meiyu front (Akiyama, 1973, 1975; Ninomiya, 1999; Kato, 1992; Kato et al., 1995; Shinoda and Uyeda, 2002; Murakami, 1959; Ninomiya and Kobayashi, 1999; Ninomiya, 2000; Lim and Kim, 2002; Moteki et al., 2004a, b; Xu et al., 2003; Ding and Hu, 2003; Yi and Xu, 2002). Shinoda et al. (2005) showed that the moist layer over mainland China is much thicker than that over the ocean during daytime, advantageous for development of the moist convection mixing layer and genesis of shallow convective clouds. Moteki et al. (2004a, b) studied the structure and development of two merging rain belts over the East China Sea by analyzing observational data, and found that there exists a "front" with a distinct gradient of humidity to the south of the Meiyu front. Zhou et al. (2005) showed that water vapor is transported from the lower troposphere to the middle and upper troposphere near the Meiyu front, and distinct gradients of water vapor exist to the north and south of the vertical transportation belt. The northern front refers to the Meiyu front and the southern one is a dew-point front with distinct humidity gradient. They named the two fronts together as the Meiyu Front System (MYFS) and found that the development of the MYFS is closely related to the intensity of Meiyu in the Jiang-Huai valley of China. Jiang and Ni (2004) also showed the existence of the MYFS and reported that an abundant water vapor supply is very important to the maintaining of the MYFS. Obviously, the distribution of water vapor has an intimate relationship with the formation of the MYFS. So far, few studies have closely and theoretically studied the formation and maintaining of the double front structure in the MYFS in the context of the distribution of water vapor. Wang et al. (2000) and Wang et al. (2002) studied the frontogenesis and interactions among moist physical processes by using theoretical models and the ARPS model respectively, and proposed a conceptual model of the interaction between cold fronts and cloud belts nearby, and they strengthened the impact of water vapor distribution. Cui et al. (2005) studied theoretically the relationship between water vapor distribution and the double front structure of the MYFS. Their results showed that the moisture gradient is more important to the formation of the double front structure than the gradient of potential temperature. In the present study, the relation between water vapor distribution and the double front structure will be further examined in the context of moisture distribution, and a tendency equation of moisture gradient will be derived to investigate the formation of the double front structure of the MYFS.

In Section 2, the relation between the double front structure of the MYFS and the distribution of atmospheric humidity will be diagnosed by using the simulation data of a torrential rain event near the MYFS in 1999. The tendency equation of moisture gradient will be proposed in Section 3, and the equation will be diagnosed by using the above simulation data so as to discuss the formation of the moisture gradient and further the MYFS in Section 4. Conclusions and discussion are given in Section 5.

2. The double front structure of the MYFS and the moisture distribution features

Cui et al. (2005) studied theoretically the relationship between the double front structure of the MYFS and the moisture distribution based on the definition of equivalent potential temperature. By applying Napierian logarithm and "∇" calculation to the definition of equivalent potential temperature, $\theta e = \theta \exp(\frac{Lq}{c_pT})$, and by a simple scaling calculation, we obtain,

$$\nabla\theta_{\mathrm{e}} = \frac{\theta_{\mathrm{e}}}{\theta}\nabla\theta + \frac{L\theta_{\mathrm{e}}}{c_pT}\nabla q, \tag{1}$$

where θ_{e}, θ, T, and q are equivalent potential temperature, potential temperature, temperature and specific humidity. $L = 2.5 \times 10^6$ J Kg^{-1} and $c_p =$ 1004 J Kg^{-1}K^{-1}. If the typical values of the atmosphere, $T = 300.0$ K, $\theta_e = 300.0$ K, $\theta = 300.0$ K, are used, Eq. (1) can be expressed as

$$\nabla\theta_e = \nabla\theta + 2500\nabla q. \tag{2}$$

As known to all, equivalent potential temperature gradients can be used to indicate the position and intensity of the MYFS (Ninomiya, 2000; Jiang and Ni, 2004). From Eqs. (1) and (2), the gradient of equivalent potential temperature is mainly related to two terms: the potential temperature gradient and the specific humidity gradient. Small variations in the specific humidity gradient can lead to large variations in the equivalent potential temperature gradient due to the bigger scaling factor (2500) in Eq. (2).

Since water vapor in the atmosphere exists mainly in the lower troposphere, the impact of the water vapor distribution and variation on the equivalent potential temperature gradient also appears mainly in the lower troposphere. In the vicinity of the Meiyu front, water vapor is transported vertically to the middle and upper troposphere, and eventually two zones of strong gradient of water vapor are formed on both sides of the water vapor vertical transportation passage (Jiang and Ni, 2004). From Eqs. (1) and (2), there will be two strong gradient zones of equivalent potential temperature corresponding to the above two strong water vapor gradient zones. The northern one is referred to as the typical Meiyu front, and the southern one is called the dew-point front (Zhou et al., 2005) or the "water vapor front" (Moteki et al., 2004a, b). These two fronts constitute the MYFS (Zhou et al., 2005) (The following analysis concludes that although the contribution of potential temperature gradient to the two strong belts of equivalent potential temperature gradient can not be overlooked, the contribution of specific humidity (water vapor) gradient is more important, at least in the region with strong gradients of water vapor).

Here a numerical simulation of a torrential rain event in the Jiang-Huai Valley of China in 1999 is analyzed and the relation between the double front structure of the MYFS and the distribution of atmospheric humidity is discussed. The model used here is the PSU/NCAR MM5 mesoscale non-hydrostatic numerical model, and the torrential rain event occurring in the Jiang-Huai Valley on 22–24 June, 1999 is simulated and analyzed. During this period, distinct torrential rainfall systems occurred and developed along the Meiyu front, leading to heavy rainfalls in the area. The MM5 model is started from 00UTC 22 June, and a 60-h simulation of the torrential rain event is carried out. Verification of the simulation (Cui et al., 2003b; Cui, 2001) showed that the MM5 model reproduces very well this torrential rain event, in cluding the development and movement of the system, the location and orientation of heavy rainfall, the upper and lower level circulations and the evolution of the Meiyu front. With regard to the detailed model setup and verification, please refer to Cui et al., (2003b) and Cui (2001). The 3-h interval coarse domain model output is used in this study. Since in MYFS, the gradient in the south-north direction is the main and most distinct component of the gradients of equivalent potential temperature, only the y component of Eq. (1) as below is diagnosed,

$$\frac{\partial\theta_e}{\partial y} = \frac{\theta_e}{\theta}\frac{\partial\theta}{\partial y} + \frac{L\theta_e}{c_pT}\frac{\partial q}{\partial y}. \tag{3}$$

Figure 1 shows the latitude-height cross sections of the three terms in Eq. (3) averaged for the simulation period. It is easy to recognize that the distribution and value of the meridional specific humidity gradient are in better agreement with those of the meridional equivalent potential temperature gradient, especially in the extreme value region. And near the Meiyu front, they have good correlation even in the middle to upper troposphere (Fig. 1b). In the Jiang-Huai Valley, the two strong meridional gradient zones of equivalent potential temperature associated with the double front structure of the MYFS are mainly contributed by the water vapor gradient term ($\frac{L\theta_e}{c_pT}\frac{\partial q}{\partial y}$), while the potential temperature gradient term ($\frac{\theta_e}{\theta}\frac{\partial\theta}{\partial y}$) has a smaller contribution, especially to the northern equivalent potential temperature gradient center (Fig. 1a). It is concluded that both potential temperature

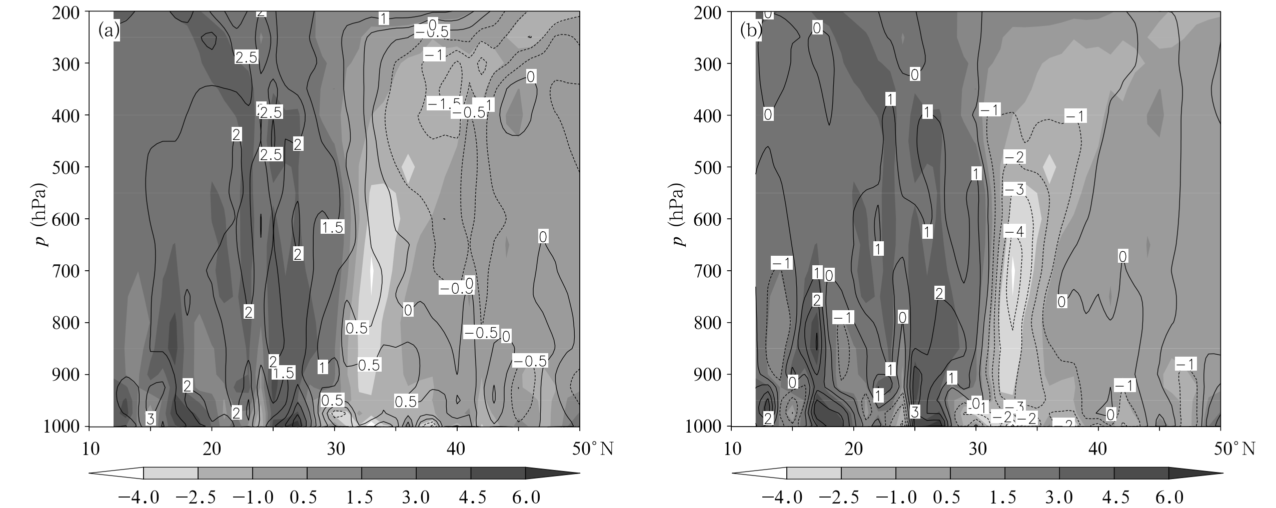

Fig.1. Time (3−57 h) averaged latitude-height cross-sections across 120°E during the model integration for (a) meridional gradients of potential temperature ($\frac{\theta_e}{\theta}\frac{\partial\theta}{\partial\theta}y$) with an interval of 0.5 in 10^{-5} K m^{-1} and (b) meridional gradients of specific humidity ($\frac{L\theta_e}{c_pT}\frac{\partial q}{\partial y}$) with an interval of 1 in 10^{-5} K m^{-1}. Shadings are meridional gradients of equivalent potential temperature in 10^{-5} K m^{-1}.

and specific humidity gradients contribute to the two strong equivalent potential temperature gradient zones indicative of the double front structure, while the specific humidity gradient is more important.

As a summary of the above analysis, the double front structure is closely related to the specific humidity gradient. Then how is the variation of the specific humidity gradient? The next section will address this issue.

3. The tendency equation of the specific humidity gradient

To analyze the variation of the specific humidity gradient, the tendency equation is derived at first.

The specific humidity equation is expressed as

$$\frac{\partial q}{\partial t}+\boldsymbol{V}\cdot\nabla q=S_v, \tag{4}$$

where S_v is the source/sink of specific humidity (water vapor), which is related to the phase change of water vapor. Cloud-resolving modeling studies (Li et al., 1999; Gao et al., 2005, 2006) indicate that S_v can be expressed as

$$S_v=-(P_{CND}+P_{DEP}+P_{SDEP}+P_{GDEP})+ P_{REVP}+P_{MLTS}+P_{MLTG}, \tag{5}$$

which includes both water and ice phase microphysics. P_{CND} is the growth of cloud water by the condensation of supersaturated vapor; P_{DEP} is the growth of cloud ice by the deposition of supersaturated vapor; P_{SDEP} and P_{GDEP} are the growth of snow and the growth of graupel by the deposition of vapor, respectively. P_{REVP}, P_{MLTS}, and P_{MLTG} are the growth of vapor by evaporation of raindrops, by evaporation of melting snow, and by evaporation of liquid from graupel surface, respectively. Applying the calculation "∇" to both sides of Eq. (4), we obtain

$$\frac{\partial\nabla q}{\partial t}+\nabla(\boldsymbol{V}\cdot\nabla q)=\nabla S_v. \tag{6}$$

Further we obtain,

$$\frac{\mathrm{d}\nabla q}{\mathrm{d}t}+\frac{\partial q}{\partial x}\nabla u+\frac{\partial q}{\partial y}\nabla v+\frac{\partial q}{\partial z}\nabla w=\nabla S_v. \tag{7}$$

Equation (7) is the tendency equation of the specific humidity gradient. To better understand the physical meaning of the equation, we further divide it into three components as below,

$$\frac{dq_x}{\mathrm{d}t}+q_x\frac{\partial u}{\partial x}+q_y\frac{\partial v}{\partial x}+q_z\frac{\partial w}{\partial x}=\frac{\partial S_v}{\partial x}, \tag{8a}$$

$$\frac{dq_y}{\mathrm{d}t}+q_x\frac{\partial u}{\partial y}+q_y\frac{\partial v}{\partial y}+q_z\frac{\partial w}{\partial y}=\frac{\partial S_v}{\partial y}, \tag{8b}$$

$$\frac{dq_z}{\mathrm{d}t}+q_x\frac{\partial u}{\partial z}+q_y\frac{\partial v}{\partial z}+q_z\frac{\partial w}{\partial z}=\frac{\partial S_v}{\partial z}, \tag{8c}$$

where $q_x = \frac{\partial q}{\partial x}$, $q_y = \frac{\partial q}{\partial y}, q_z = \frac{\partial q}{\partial z}$, and Eq. (8) can be further expressed as,

$$\frac{dq_x}{\partial t} = \frac{\partial S_v}{\partial x} - \boldsymbol{V} \cdot \nabla q_x - (q_x \frac{\partial u}{\partial x} + q_y \frac{\partial v}{\partial x} + q_z \frac{\partial w}{\partial x}), \tag{9a}$$

$$\frac{dq_y}{\partial t} = \frac{\partial S_v}{\partial y} - \boldsymbol{V} \cdot \nabla q_y - (q_x \frac{\partial u}{\partial y} + q_y \frac{\partial v}{\partial y} + q_z \frac{\partial w}{\partial y}), \tag{9b}$$

$$\frac{dq_z}{\partial t} = \frac{\partial S_v}{\partial z} - \boldsymbol{V} \cdot \nabla q_z - (q_x \frac{\partial u}{\partial z} + q_y \frac{\partial v}{\partial z} + q_z \frac{\partial w}{\partial z}). \tag{9c}$$

Equation (9) shows that the local change of the specific humidity gradient is closely related to the advection, convergence/divergence, secondary circulation effects, and source/sink effect of water vapor (cloud microphysical processes). Since the meridional gradient is the main component of the gradient of equivalent potential temperature related to the MYFS, the analysis below will focus on Eq. (9b). From Eq. (9b), it is noted that the local change of the meridional specific humidity gradient is closely related to the advection of meridional specific humidity gradient, the horizontal vorticity effect $(-q_x \frac{\partial u}{\partial y})$, the meridional convergence/divergence $(-q_y \frac{\partial v}{\partial y})$, the meridional secondary circulation $(-q_z \frac{\partial w}{\partial y})$ and the meridional distribution of source/sink of water vapor $(\frac{\partial S_v}{\partial y})$.

4. Diagnostic analysis of the double front structure

In this section, the variation of the double front structure of the MYFS will be diagnosed by using the simulation data and Eq. (9).

To discuss the evolution of the double front structure, that is, the frontogenesis/frontolysis, we here follow the definition of the frontogenetical function proposed by Ninomiya (1984): both sides of Eq. (9b) are multiplied by q_y,

$$\underbrace{q_y \frac{\partial q_y}{\partial t}}_{A} = q_y \frac{\partial S_v}{\partial y} \underbrace{- q_y(\boldsymbol{V} \cdot \nabla q_y)}_{B} \underbrace{- q_x q_y \frac{\partial u}{\partial y}}_{C} \underbrace{- q_y q_y \frac{\partial v}{\partial y}}_{D} \underbrace{- q_y q_z \frac{\partial w}{\partial y}}_{E}. \tag{10}$$

The left side of Eq. (10) represents the local change of the absolute value of the meridional specific humidity gradient, and the right side represents different contributions. Here A is used to denote the term on the left side of Eq. (10). It represents the evolution of the double front structure, i.e., the frontogenesis or frontolysis. B is the advection term of specific humidity gradient. C represents the horizontal vorticity effect (deformation or twisting effect). D is the meridional convergence/divergence (or deformation) effect. E represents the secondary circulation effect. The meridional gradient of source/sink of water vapor $(q_y \frac{\partial S_v}{\partial y})$ in Eq. (10) will be only diagnosed and discussed indirectly $(q_y \frac{\partial S_v}{\partial y} = A - (B + C + D + E))$ because the model output does not contain detailed microphysical data.

Firstly, the contribution of the source/sink of water vapor $(q_y \frac{\partial S_v}{\partial y})$ is analyzed qualitatively. In Eqs. (4) and (5), S_v represents the individual change of specific humidity caused by the phase change of water vapor. In the vicinity of the Meiyu front, torrential rainfall systems (raining cloud systems) develop and move close to the front (Cui et al., 2003b). Figure 2 shows time (3−57 h) averaged latitude-height cross sections across 120°E during the model integration, in which the rainfall and cloud systems always evolve along the equi-scalar surface of equivalent potential temperature of the Meiyu front. As we know, the development of rainfall systems has a close relation with the phase change of water vapor, so nearby the rainfall systems, S_v shows a distinct variation. When the systems develop strongly, S_v often decreases to the south of the Meiyu front and increases towards the north, so

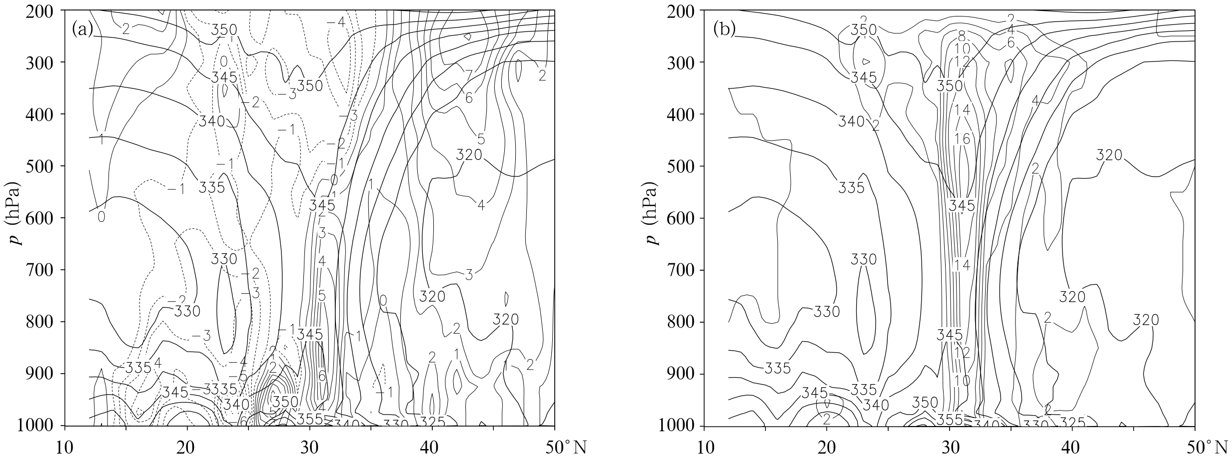

Fig.2. Time (3–57 h) averaged latitude-height cross-sections across 120°E during the model integration of (a) vertical component of relative vorticity (ς_z) (thin lines with an interval of 1.0 and a unit of 10^{-5} s^{-1}) and (b) sums of mixing ratios of simulated hydrometeors (cloud water, rain water, and so on) (thin solid lines with an interval of 2 and a unit of 10^{-5} Kg Kg^{-1}). Bold solid lines are equivalent potential temperature (K).

we get $q_y \dfrac{\partial S_v}{\partial y} < 0$ (q_y <0). And according to Eq.(10), we get $q_y \dfrac{\partial q_y}{\partial t} < 0$, that is, frontolysis will appear there.

Figure 3 shows time (3–57 h) averaged latitude-height cross sections across 120°E of the vrious terms in Eq.(10) during the model integration. The source/sink term of water vapor, as mentioned above, is diagnosed indirectly by $q_v \dfrac{\partial S_v}{\partial y} = A-(B+C+D+E)$. In the context of time mean, most of the variations of the absolute value of the meridional specific humidity gradient appear in the vicinity of the northern front, that is, near the Meiyu front. Vertically, the variations mainly exist below 600 hPa and there are two extreme value centers near 700 and 900 hPa, respectively, with the center near 700 hPa stronger (Fig. 3a), which tells that distinct frontogenesis appears in the Meiyu front during the simulation. Since the Meiyu front lies in the region where interactions happen between cold, dry air and warm, moist air and between the front and mesoscale torrential rainstorms, the distinct change of gradients and the occurrence of frontogenesis (frontolysis) are expectable. From Figs. 3b–f, it is seen that the change mainly comes from the meridional convergence/divergence effect $(-q_y q_y \dfrac{\partial v}{\partial y})$, the meridional secondary circulation effect $(-q_z q_y \dfrac{\partial w}{\partial y})$ and the source/sink effect of water vapor $(q_y \dfrac{\partial S_v}{\partial y})$.

The meridional convergence/divergence effect $(-q_y q_y \dfrac{\partial v}{\partial y})$ exists mainly in the middle and lower troposphere below 500 hPa. There are two positive value centers near 700 and 900 hPa with the center near 700 hPa being stronger, suggesting that distinct meridional convergence exists there $(\dfrac{\partial v}{\partial y} < 0)$, leading to stronger meridional frontogenesis. The two centers near 700 and 900 hPa correspond to the two centers in Fig.3a, which tells that the meridional convergence/divergence is very important to the meridional frontogenesis of the Meiyu front. The meridional secondary circulation effect (Fig. 3e) counteracts part of the impact of the source/sink effect of water vapor (Fig. 3f), and both show extreme value centers near 700 hPa, corresponding to the centers of A and D terms in Eq.(10). This tells that they all have important contributions to the change of the meridional gradient of specific humidity. The simple diagnostics here gives similar results as the previous discussion on the source/sink effect of water vapor. In the vicinity of the Meiyu front, especially between the rainfall systems and the front, the source/sink effect leads to negative A, that is, negative change of the absolute value of the meridional specific humidity gradient,

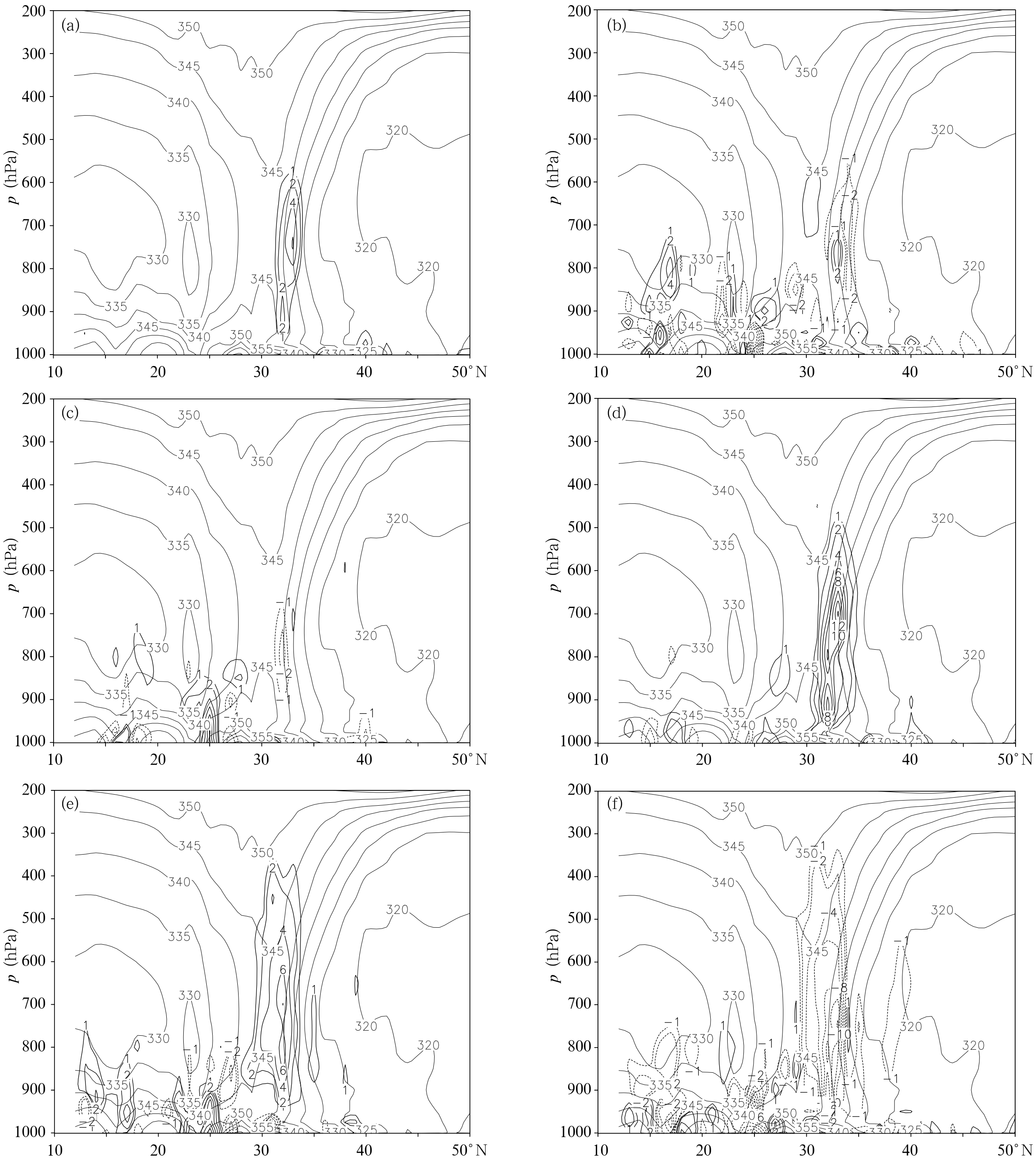

Fig.3. Time (3−57 h) averaged latitude-height cross-sections across 120°E during the model integration for (a) local variation of the meridional gradient of specific humidity ($q_y\dfrac{\partial q_y}{\partial t}$), (b) advection term ($-q_v(\boldsymbol{V}\cdot\nabla q_y)$), (c) vertical vorticity term ($-q_x q_y\dfrac{\partial u}{\partial y}$), (d) meridional convergence term ($-q_y q_y\dfrac{\partial v}{\partial y}$), (e) meridional secondary circulation term $-q_z q_y\dfrac{\partial w}{\partial y}$, and (f) $A-(B+C+D+E)$, the source/sink term of water vapor ($q_y\dfrac{\partial S_v}{\partial y}$). Thin solid lines are equivalent potential temperature in K, and bold lines are for the terms in Eq. (10) in 10^{-21} Kg Kg^{-1} m^{-1} s^{-1}.

and further negative change of the absolute value of the meridional equivalent potential temperature gradient. Eventually frontolysis takes place in the Meiyu front. The above analysis shows that there are three terms having great impacts on the meridional frontogenesis of the Meiyu front: the meridional convergence effect and the secondary circulation effect exert positive impacts on the frontogenesis, while the source/sink effect of water vapor exerts a negative impact on the frontogenesis.

In this article, only the time mean characteristics of a torrential rain event are examined and presented, and only the meridional frontogenesis and frontolysis are discussed. In different stages of synoptic systems' development, on different height levels, owing to the difference of the interaction between cold, dry air and warm, moist air, and the interaction between the Meiyu front and torrential rainstorms, contributions of the above effects will give different results. To inspect comprehensively and in detail the frontogenesis/frontolysis processes, and to study closely the interaction between the Meiyu front and torrential rainstorms, it is necessary to discuss and study the frontogenesis/frontolysis in different directions and in different stages by using simulation data and the above equations. These will be addressed in another paper.

5. Conclusions and discussion

The double front structure and the distributions of the equivalent potential temperature, potential temperature and specific humidity in the Jiang-Huai valley are studied by diagnosing high-resolution simulation data of a torrential rain event in 1999 with MM5. The results show that, both potential temperature and specific humidity gradients have impacts on the formation of the double front structure of the MYFS, while the specific humidity gradient is more important. A tendency equation of the specific humidity gradient is proposed and diagnosed by using the mesoscale simulation data. The results show that the change of the specific humidity gradient is related to advection effect, convergence/divergence effect, horizontal or vertical vorticity (secondary circulation) effects and the gradient of the source/sink of water vapor. Time mean analysis shows the change of the meridional specific humidity gradient is mainly caused by the meridional convergence/divergence effect, the meridional secondary circulation effect and the source/sink effect of water vapor, among which the convergence/divergence effect exerts a more distinct impact on frontogenesis in the vicinity of the Meiyu front, and the source/sink effect of water vapor exerts an inverse impact than the convergence/divergence and the meridional secondary circulation effects, leading to frontolysis. Since the source/sink of water vapor is closely related to the phase change, and is further related to cloud microphysics, the change of specific humidity gradient is then closely related to cloud microphysics and further related to the evolution of rainfall systems and clouds.

The current study shows that the distributions of the two belts with strong equivalent potential temperature gradient in the Jiang-Huai Valley related to the double front of the MYFS are closely related to the distribution of the specific humidity gradient. The distribution of water vapor in the atmosphere is very important to the maintaining of the double front (Jiang and Ni, 2004). The tendency equation of the specific humidity gradient can be used to study the change of the distribution of water vapor and further the change of the equivalent potential temperature gradient to understand the evolution of the double front.

As known to us, the MYFS has a close relationship with raining cloud systems and relevant torrential rainfall systems (Cui et al., 2003b). The MYFS provides a favorite environment for the torrential rainfall systems (including instability, abundant water vapor supply and lifting mechanism) to develop and move in the vicinity of the Meiyu front (Cui et al., 2003b; Wu and Liu, 1998). In turn, the development of torrential rainfall systems exerts impacts on the Meiyu front (frontogenesis or frontolysis) by heat and mass forcing (Gao et al., 2002; Cui et al., 2003a, b; Cui, 2001). The comprehensive understanding of the interaction between the Meiyu front and torrential rainfall systems is very important to our further understanding and predicting of the rainfall processes near the MYFS (Wang et al., 2002). By using vorticity equation (Cui et al., 2003b) and the above tendency equation of the specific humidity gradient or frontogenetical function equation (Ninomiya, 1984), we can discuss the interaction between the MYFS and torrential rainfall systems. The tendency equations in this article, Eqs. (9b) and (10), depict the main problem in the MYFS (the important influence of the distribution of water vapor), and connect the frontogenesis/frontolysis with the cloud microphysics near the Meiyu front through the gradient of water vapor, showing some advantages in the study of torrential rainfall events near the MYFS.

Here only one torrential rainfall case is selected and diagnosed. Since cases may differ, it is necessary to conduct more case studies.

REFERENCES

Akiyama, T., 1973: The large-scale aspects of the characteristic features of the Baiu Front. *Pap. Meteor. Geophys.*, **24**, 157–188.

Akiyama, T., 1975: Southerly transversal moisture flux into the extremely heavy rainfall zone in the Baiu season. *J. Meteor. Soc. Japan*, **53**, 304–316.

Cui Xiaoping, 2001: Study on slantwise vorticity development of subtropical cyclones (PhD thesis). Institute of Atmospheric Physics, Chinese Academy of Sciences, Beijing, 146 pp. (in Chinese)

Cui X., Gao S., and Wu G., 2003a: Moist potential vorticity and up-sliding slantwise vorticity development. *Chin. Phys. Lett.*, **20**, 167–169.

Cui X., Gao S., and Wu G., 2003b: Up-sliding slantwise vorticity development and the complete vorticity equation with mass forcing. *Adv. Atmos. Sci.*, **20**, 825–836.

Cui X., Gao S., Zong Z., Liu W., and Li X., 2005: Physical mechanism of formation of the bimodal structure in the Meiyu front system. *Chin. Phys. Lett.*, **22**, 3218–3220.

Ding Yihui and Hu Guoguan, 2003: A study on water vapor budget over china during the 1998 severe flood periods. *Acta Meteor. Sinica*, **61**, 129–145. (in Chinese)

Gao S., Tao S., and Ding Y., 1990: The generalized E-P flux of wave-mean flow interactions. *Sci. Chin. (Series B)*, **33**, 704–715.

Gao S., Lei T., and Zhou Y., 2002: Moist potential vorticity anomaly with heat and mass forcings in torrential rain systems. *Chin. Phys. Lett.*, **19**, 878–880.

Gao S., Cui X., Zhu Y., Li X., and Tao W.-K., 2005: A Modeling Study of Moist and Dynamic Vorticity Vectors Associated with 2D Tropical Convection. *J. Geophys. Res.*, **110**, D17104, doi:10.1029/2004JD005675.

Gao S., Ping F., Cui X., and Li X., 2006: Short Timescale Air-Sea Coupling in the Tropical Deep Convective Regime. *Meteor. Atmos. Phys.* 93, 37–44, DOI 10.1007 /s00703-005-0161-8

Jiang J., and Ni Y., 2004: Diagnostic study on the structural characteristics of a typical Mei-yu front system and its maintenance mechanism. *Adv. Atmos. Sci.*, **21**, 802–813.

Kato, K., 1992: Synoptic features on moisture field and shallow convection in the subtropical high area around Japan in early July of 1988. *J. Meteor. Soc. Japan*, **70**, 757–768.

Kato, K., J. Matsumoto, and H. Iwasaki, 1995: Diurnal variation of cb-clusters over China and its relation to large-scale conditions in the summer of 1979. *J. Meteor. Soc. Japan*, **73**, 1219–1234.

Li X., Sui C.-H., Lau K.-M., and Chou M.-D., 1999: Large-Scale Forcing and Cloud-Radiation Interaction in the Tropical Deep Convective Regime. *J. Atmos. Sci.*, **56**, 3028–3042.

Lim, Y.-K., and Kim K.-Y., 2002: Temporal and spatial evolution of the Asian summer monsoon in the seasonal cycle of synoptic fields. *J. Climate*, **15**, 3630–3644.

Matsumoto, S., S. Yoshizumi, and M. Takeuchi, 1970: On the structure of the Baiu front and associated intermediate-scale disturbances in the lower atmosphere. *J. Meteor. Soc. Japan*, **48**, 479–491.

Matsumoto, S., K. Ninomiya, and S. Yoshizumi, 1971: Characteristic features of Baiu front associated with heavy rainfall. *J. Meteor. Soc. Japan*, **49**, 267–281.

Moteki, Q., H. Uyeda, T. Maesaka, T. Shinoda, M. Yoshizaki, and T. Kato, 2004a: Structure and development of merged two rainbands observed over East China Sea during X-BAIU-99. Part I: Meso-β-scale structure and development processes. *J. Meteor. Soc. Japan*, **82**, 19–44.

Moteki, Q., H. Uyeda, T. Maesaka, T. Shinoda, M. Yoshizaki, and T. Kato, 2004b: Structure and development of merged two rainbands observed over East

China Sea during X-BAIU-99. Part II: Meso-α-scale structure and build-up processes of convergence in the Baiu frontal region. *J. Meteor. Soc. Japan*, **82**, 45–65.

Murakami, T., 1959: The general circulation and water-vapor balance over the Far East during the rainy season. *Geophys. Mag.*, **29**, 131–171.

Ninomiya, K., 1984: Characteristics of Baiu front as a predominant subtropical front in the summer Northern Hemisphere. *J. Meteor. Soc. Japan*, **62**, 880–894.

Ninomiya, K., and C. Kobayashi, 1999: Precipitation and moisture balance of the Asian summer monsoon in 1991. Part II: Moisture transport and moisture balance. *J. Meteor. Soc. Japan*, **77**, 77–99.

Ninomiya, K., 1999: Moisture balance over China and the South China Sea during the summer monsoon in 1991 in relation to the intense rainfalls over China. *J. Meteor. Soc. Japan*, **77**, 737–751.

Ninomiya, K., 2000: Large- and meso-α-scale characteristics of Mei-yu/Baiu front associated with intense rainfalls in 1–10 July 1991. *J. Meteor. Soc. Japan*, **78**, 141–157.

Ni Yunqi and Zhou Xiuji, 2004: Study for formation mechanism of heavy rainfall within the Meiyu front along the middle and downstream of Yangtze river and theories and methods of their detection and prediction, *Acta Meteor. Sinica*, **62**, 647–662. (in Chinese)

Qin D., Jiang J., and Fang Z., 2004: The characteristics of water vapor plume in the heavy rain events during 21–24 June 2002. *Acta Meteor. Sinica*, **62**, 329–337. (in Chinese)

Shou S., Li Y., and Fan K., 2001: Isentropic potential vorticity analysis of the mesoscale cyclone development in a heavy rain process. *Acta Meteor. Sinica*, **59**, 560–568. (in Chinese)

Shinoda, T., and Uyeda H., 2002: Effective factors in the development of deep convective clouds over the wet region of eastern China during the summer monsoon season. *J. Meteor. Soc. Japan*, **80**, 1395–1414.

Shinoda, T., H. Uyeda, K. and Yoshimura, 2005: Structure of moist layer and sources of water over the southern region far from the Meiyu/Baiu front. *J. Meteor. Soc. Japan*, **83**, 137–152.

Wu G., and Liu H., 1998: Vertical Vorticity development owing to down-sliding at slantwise isentropic surface. *Dynamics of Atmospheres and Oceans*, **27**, 715–743.

Wang, Y., Wu R., and Pan Y., 2000: Evolution and frontogenesis of an imbalanced flow-the influence of vapor distribution and orographic forcing. *Adv. Atmos. Sci.*, **17**, 256–274.

Wang, C., Wu R., and Wang Y., 2002: Interaction of diabatic frontogenesis and moisture processes in cloud-frontal rain-band. *Adv. Atmos. Sci.*, **19**, 544–561.

Xu X., Miao Q., Wang J., et al., 2003: Transport model at the regional boundary during the Meiyu period. *Adv. Atmos. Sci.*, **20**, 333–342.

Yi Q. and Xu X., 2002: The propagation and development of cloud cluster systems and severe precipitation event in 1998. *Climatic and Environmental Research*, **6**,129–145. (in Chinese)

Yan J., Wu G., and Cui X., 2005: Comparison of Two Kinds of Atmospheric Vorticity Equations. *Chin. Phys. Lett.*, **22**, 769–772.

Zhou Y., Gao S., and Samuel S.P. Shen, 2005: A diagnostic study of formation and structures of the MYFS over East Asia. *J. Meteor. Soc. Japan*, **82**, 1565–1576.